Measurement of moisture content in a fluidized bed dryer using an electrostatic sensor array

Wenbiao Zhang[1], Xufeng Cheng[1], Yonghui Hu[1] and Yong Yan[1,2] *

[1] School of Control and Computer Engineering, North China Electric Power University, Beijing 102206, China

[2] School of Engineering and Digital Arts, University of Kent, Kent CT2 7NT, UK

* Corresponding author E-mail: y.yan@kent.ac.uk

Abstract

Fluidized bed dryers have been widely applied to dry raw materials or final products due to the advantages of good mixing efficiency and high heat and mass transfer rate. In order to control and optimize the drying process of fluidized bed dryers, it is necessary to develop reliable methods to measure the moisture content of solid particles in the bed. Because of the advantages of non-intrusiveness, simple structure and high sensitivity, an electrostatic sensor array has been developed to monitor the drying process. Experimental investigations were conducted on a lab-scale fluidized bed dryer. The moisture content during the drying process was measured using the sampled particles as reference. It is found that the fluctuation of the electrostatic signals can reflect the change in moisture content. However, the relationship between the fluctuation of the electrostatic signal and the moisture content depends on the air velocity in the dryer. To eliminate the velocity effect on moisture content measurement, a model between the moisture content and the root-mean-square magnitude of the electrostatic signal is established. The effectiveness of the model is validated using experimental results under a range of conditions. The findings indicate that the electrostatic sensor array can measure the moisture content in the bed with a maximum error of ±15%.

Keywords: *Fluidized bed; drying; moisture content; electrostatic sensor; sensor array; measurement*

Nomenclature

A_{rms}	RMS value of the electrostatic signals (V)
a	Coefficient (-)
b	Coefficient (-)
I_{ind}	Induced electrostatic current (A)
P_i	Predicted value (wt. %)
q_m	Particle charge-to-mass ratio (C/kg)
S_i	Sampled value (wt. %)
T	Inlet air temperature (^oC)
u_b	Bubble riser velocity (m/s)
v_a	Superficial air velocity (m/s)
v_c	Correlation velocity (m/s)
X	Moisture content.
X_0	Initial moisture content.

1. Introduction

Owing to the advantages of good mixing efficiency and high heat and mass transfer rates, fluidized bed dryers (FBDs) have been widely applied in chemical engineering processes to remove the moisture content (i.e. the weight of water over the total weight of the particles) from raw materials or final products [1]. The control and optimization of the FBDs are important to improve the product quality and reduce the energy consumption. For example, drying beyond the end point will increase the frictions between particles, result in more powders and affect the quality of the final products. In order to control the drying process, reliable methods to measure the moisture content and flow behavior of the solid particles are needed [2].

There are many types of methods available for the measurement of moisture content and flow behavior of solid particles in the FBDs, including pressure fluctuation [3-4], acoustic emission [5-8], electrical capacitance tomography (ECT) [9-12], microwave resonance [13] and triboelectric probes [14-16]. Aghbashlo *et al*. presented a review on the techniques to monitor and control the fluidization quality in the FBDs [17]. The advantages and disadvantages of each technique for moisture content and flow behavior measurement were presented and the prospects for future research in this area were also identified in the review.

Electrification is inevitable in particulate processes due to the contact and frictions between particles and the collisions between the particles and the wall. The charging characteristics of solid particles is influenced by many factors, such as size, velocity and concentration of solid particles, work function, initial charging state and moisture content. Park *et al*. found that the charges on particles were reduced with the increase of moisture content of the fluidization air [18]. The higher moisture content enhanced the conductivity of solid particles and increased the charge dissipation rate. In addition, Giffin and Mehrani analyzed the effect of air humidity on the wall fouling of the bed due to particle electrification and found that the extent of wall fouling was reduced with higher humidity [19]. The effects of moisture content on the mass flow measurement of pneumatically conveyed particles using electrostatic sensors were investigated by Qian *et al*. [20]. Taghavivand *et al*. investigated the drying kinetics and tribocharging behavior of pharmaceutical particles in a fluidized bed dryer [21]. It was concluded that the charge on the particles is a direct indication of the moisture content and the

dynamic charge can be used to monitor the drying process. Because of the significant influence of the moisture content on particle charging, intrusive probes and non-intrusive electrodes based on the triboelectic effect and electrostatic induction can be applied to measure the moisture content in the FBDs. Portoghese *et al*. used triboelectic probes to monitor the liquid concentration and the moisture content in wet fluidized bed [14, 15]. It was found that the electrostatic signal is sensitive to the moisture content below 100 ppm. Triboelectric probes were also applied to monitor the mixing and drying process in a vibrated fluidized bed [16]. However, intrusive probes cannot be installed in food and medicine production processes, which deteriorate the quality of the final products.

In order to ensure the quality of the final products, it is desirable to develop a non-intrusive method for the measurement of moisture content in FBDs. Electrostatic sensing has the advantages of low cost, high sensitivity and fast response. This paper presents the application of a non-intrusive electrostatic sensor array to measure the moisture content in the FBD. The drying kinetics of solid particles in a lab-scale FBD is investigated by changing the superficial air velocity and the inlet air temperature. The relationship between the moisture content and the characteristics of the electrostatic signal is established and then used for on-line continuous measurement of moisture content in the FBDs.

2. Measurement method

2.1. Electrostatic sensor array

Based on the principle of electrostatic induction, electrostatic sensor arrays have been applied to measure the flow parameters of solid particles in pneumatic conveying pipelines [22, 23] and fluidized beds [24-26]. However, there has been no report on the application of electrostatic sensors to measure the moisture content in FBDs. As a non-intrusive method, the electrostatic senor arrays are installed on the bed wall and the electrodes are strategically mounted to measure the moisture content. As shown in Figure 1, the electrostatic sensor array used in this study includes four sets of electrodes, which are labeled as A, B, C and D, respectively. Three identical electrodes are included in each set. The distance between the adjacent electrodes should be reasonably small to maintain good similarity between the two signals. Since the inner diameter of the FBD used in the present study is 180 mm, the distance between the two adjacent electrodes is set to 20 mm. In consideration of the amplitude and bandwidth

of the signal, the width of each electrode is set to 6 mm. The central angle of the electrode is 60 degree. The electrodes are made of copper and tightly wrapped around the outer surface of the bed. The thickness of the wall is 5 mm and the relative permittivity of the material is 2.3. The permittivity of the material and the thickness of the wall will affect the capacitance between the charged particles and the electrode, which will further affect the induced charge on the electrode. Through the analysis of the sensitivity distribution of the electrode [24], it has been found that the electrode is more sensitive to charged particles closer to the electrode, which can provide localized flow information in the bed. With the application of the sensor array, the moisture content and the flow behavior of the solid particles in different parts of the FBD are obtained.

Figure 1. Electrostatic sensor array.

2.2. Moisture content measurement

The signal conditioning and processing procedure of the electrostatic sensor array is illustrated in Figure 2. With the movement of solid particles and the fluctuation of the charges, a change in electrical current is detected on the electrode. The current signal is converted into a voltage signal through a preamplifier and then the signal is fed into a second-order low-pass filter with a cut-off frequency of 1000 Hz, which is enough for the dynamic response of the measurement system. Finally, the signal is further amplified through a gain adjustable amplifier. The schematic of the signal conditioning circuit is available in [25]. A grounded metal box was installed outside the electrodes and the circuit boards in order to eliminate external electrical interference and enhance the signal-to-noise ratio.

He *et al.* [28, 29] proposed the relationship among the induced electrostatic current, the particle charge-to-mass ratio and the bubble rise velocity

$$I_{ind} = -0.17 q_m u_b^{1.1} \tag{1}$$

where I_{ind} represents the induced electrostatic current, q_m stands for the particle charge-to-mass ratio and u_b represents the bubble rise velocity. The moisture content affects the particle charge-to-mass ratio and hence the induced electrostatic current. In order to measure the moisture content using the electrostatic signals, correlation velocity of the particles is calculated. Since the flow behavior in the FBD is very complex and the flow parameters fluctuate significantly, the correlation velocities from

the three electrodes are fused to calculate a more reliable result [25]. Besides, the root-mean-square (RMS) magnitude is used as an indicator of the signal fluctuation. With the knowledge of the correlation velocity and the RMS magnitude of the electrostatic signal, a predictive model for the moisture content is built. As a result, a method for measuring moisture content in the FBDs using electrostatic sensor array is proposed.

Figure 2. Signal conditioning and processing procedure of the electrostatic sensor array.

3. Experimental setup

Experiments on moisture content measurement were conducted in a lab-scale FBD. Figure 3 shows the experimental setup of the lab-scale FBD, with a temperature and humidity sensor and an electrostatic sensor array installed on the dryer. The material of the FBD is Plexiglas and the inner diameter and the height of the bed are 180 mm and 1000 mm, respectively. The distributor plate used in fluidized bed was made of a thick aluminum plate drilled with 3 mm-diameter holes, giving an opening area of 5%. Fluidization air was generated from a blower and it was heated to a desirable temperature using an electrical heater. The temperature (T) of the hot air was set to 45, 60 and 75 ^{o}C, respectively and the corresponding relative humidity at the inlet of the FBD was found to range from 4% to 5%. The air flow rate was regulated by a vent valve behind the blower and it was measured by a vortex flow meter (accuracy 1.5%). The superficial air velocity (v_a) was set from 0.44 m/s to 0.67 m/s in order to operate in a bubbling fluidization regime and reduce the entrainment of the fine powders from the FBD. The Test Conditions (TC) of the fluidized bed dryer under different inlet air velocities and air temperatures are summarized in Table 1. The solid material used in the experiment was corn particles. The images of the corn particles were captured using a self-developed image acquisition system [30]. The size distribution of the particles was calculated through off-line processing of the images. It is found that the particle size is mainly from 1 mm to 1.8 mm, as shown in Figure 4. The true density of the particles is 1.1 g/cm^3, which is provided by the supplier of the material. As a result, the corn particles are considered as Geldart D particles.

Figure 3. Experimental setup of the fluidized bed dryer.

Table 1. Experimental conditions of the fluidized bed dryer under different inlet air velocities and air temperatures

Figure 4. Size distribution of the corn particles.

The temperature and humidity sensor (Model HMP110, Vaisala) was installed at the outlet of the bed to measure the temperature and relatively humidity of the exhaust air. The electrostatic sensor array for moisture content measurement was installed 200 mm above the distributor.

Before the start of the experiments, the moisture content of the original particles was measured and they were mixed with water by a mixer to a desirable moisture content. The wet particles were kept in an air tight container for at least 6 hours to ensure uniformity of the moisture content within. Nearly 8 kg wet particles were prepared in each experiment and added to the bed, forming a static bed height of 415 mm. As a result, the electrostatic sensor array was in the dense phase region of the FBD, where the cross-sectional distribution of the solid particles is relative uniform and the fluctuation of the electrostatic signal is not influenced by the spatial distribution of the particles. The heated air was used to dry the solid particles in the FBD and the corn particles were sampled from a sampling port (170 mm above the sensor array) into a sealed glass vial every 5 minutes after the start of drying. When the particles were sampled, the signals from the temperature and humidity sensor and the electrostatic sensor array were recorded simultaneously for 60 seconds using a data acquisition device (Model USB-6363, National Instruments). The moisture content of the sampled corn particles was measured using a Halogen Moisture Analyzer (Model HE83, METTLER TOLEDO). The solids moisture at different times was recorded during the drying process for further investigations.

4. Results and discussion

4.1. Outlet air temperature, relative humidity and moisture content

In practice, the temperature and relative humidity of the exhaust air are key parameters to monitor in the drying process. Figure 5 shows the representative time histories of the temperature and relative humidity of the outlet air during the drying process under the experimental condition of TC3. It can be seen that the relative humidity of the outlet air increases to a nearly saturated value (95%) at the beginning of the drying because the moisture on the particle surface evaporates into the air. After that,

the relative humidity of the outlet air gradually decreases as the surface of the particle becomes dry. Meanwhile, it is found that the temperature of the outlet air gradually increases during the drying process.

Figure 5. Temperature and relative humidity of the exhaust air during the drying process under the experimental condition of TC3.

In the batch drying of solids, the drying rate experiences two phases: the constant drying rate phase and the falling rate phase [31]. The surface moisture on the particle and water in large pores of the particle predominantly influences the constant drying rate, whereas the moisture, which is trapped or bound within the solids, controls the falling rate. The time histories of moisture content under the different conditions are given in Figure 6. It is found that the solids drying is at the constant drying rate phase and the drying rate increases with the air temperature and the air velocity. In addition, the particles reach the equilibrium moisture content of 6 wt. % after drying for 2 hours.

Figure 6. Time histories of moisture content under different conditions.

4.2. Electrostatic signals

Figure 7 plots the electrostatic signals from the three electrodes in set A during the drying process under the experimental condition of TC3, which are labeled as A-1, A-2 and A-3 from low to high positions. The three signals from the electrodes exhibit similar patterns with consistent delays between each other. It is observed that at the beginning of the drying process (Figure 7 (a)), the electrostatic signal is weak due to the high moisture on the particles and enhanced charge dissipation rate. In addition, the channeling was observed at the beginning of the drying process and the solid particles were not fluidized, resulting in less charge generated. This phenomenon disappeared with the progress of drying and smooth fluidization was found. The moisture content became lower and the electrostatic charges on the particles increased with the drying time. As a result, the fluctuation of the electrostatic signal became stronger, as shown in Figure 7 (b) and (c). However, by comparing the electrostatic signals from Figure 7 (c) and (d), it is found that, after 100 min drying, the electrostatic signals present less fluctuations. Based on the above analysis, it is concluded that the fluctuation of the electrostatic

signal is sensitive to the change of moisture content.

Figure 7. Electrostatic signals from electrodes A-1, A-2 and A-3 during the drying process under the experimental condition of TC3.

In the electrostatic sensor array, twelve electrodes are installed at different positions of the FBD. The fluctuations of electrostatic signals from different electrodes are associated with the charging characteristics of the corn particles in the FBD during the drying process. In order to investigate the electrostatic charge distribution in the FBD during the drying process, the RMS magnitudes of the electrostatic signals from the three electrodes in set A, are calculated, as shown in Figure 8. The RMS value of each electrode is calculated based on the electrostatic signal with a duration of 60 seconds. The time histories of the RMS magnitudes during the drying process can be divided into three parts, which are labeled as parts I, II and III. In part I, due to the channeling effect between wet particles, the corn particles in the FBD were not fluidized and the fluctuations of the electrostatic signals were weak. With the progress of the drying, the moisture on the particles became lower. The corn particles were fluidized with the movement of the bubbles in the FBD and the flow behavior in the FBD became turbulent, which resulted in the increase of the RMS values. In addition, by comparing the RMS values of the signals from the three electrodes, it is found that the signal from electrode A-3 is higher in magnitude than those from electrodes A-1 and A-2, which suggests that there are more charges on the particles in the higher position of the FBD. However, in part III, based on the investigation of Taghavivand *et al.* [21], when the particles reached the equilibrium moisture content, the charge on the particles arrived at its equilibrium value. Since the electrostatic signal is generated by the induction of the charge on the particles, when the charge on the particles reaches its equilibrium value, the electrostatic signals present less fluctuations and the RMS values of the signals decrease.

Figure 8. RMS values of the electrostatic signals from set A electrodes during the drying process under the experimental condition of TC3.

In order to represent the charging characteristics in the FBD, the average RMS values of the electrostatic signals from the twelve electrodes during the drying process are calculated. The relationships between the average RMS value and the moisture content under the same air velocity

with different inlet air temperatures are given in Figure 9. With the decrease of the moisture content from 18% to 10% on weight, the RMS value of the electrostatic signal increases to nearly 1.6 V. It is well known that the RMS value of the electrostatic signal depends strongly on the air velocity in the bed. The relationships between the average RMS value of the electrostatic signals and the moisture content under the same inlet air temperature with different air velocities are also investigated, as shown in Figure 10. It is found that under the same moisture content, the average RMS value increases with the air velocity. In comparison with the influence of the inlet air temperature on the relationship between the RMS value and the moisture content, the effect of the air velocity is more obvious. Taghavivand *et al.* found that the electrostatic charge on the pharmaceutical granules was a function of moisture content and drying air velocity, rather than drying air temperature, which proves the results in Figures 9 and 10 [21]. Since it is difficult to decouple the effect of velocity from that of moisture content, the velocity effect should be considered in order to accurately predict the moisture content based on the fluctuation of the electrostatic signal.

Figure 9. Relationships between the average RMS value of the electrostatic signals and the moisture content under the air velocity of 0.52-0.57 m/s with different inlet air temperatures.

Figure 10. Relationship between the average RMS value of the electrostatic signals and the moisture content under the same inlet air temperature of 60 ^{o}C with different air velocities.

4.3. Correlation velocity in the FBD

Although the correlation velocity is not the same as the actual solids velocity, it can represent the solids motion in the FBD. By cross-correlating the electrostatic signals from adjacent electrodes, a weighted average velocity is obtained by fusing the correlation velocities with their correlation coefficients. The weighted average velocities from different electrode sets under moisture content of 12.2 wt. % are shown in Figure 11. It is observed that there is a relative uniform velocity profile in the FBD when the wet particles are fluidized. By averaging the weighted average velocities from different electrode sets, the spatial-averaged correlation velocity during the drying process when the superficial air velocity is 0.48 m/s is given in Figure 12. At the beginning of drying, due to the high moisture content and channeling effect between particles, the solids particles in FBD are not fluidized. With the

progress of the drying process, the moisture content decreases and the channeling effect weakens, thus the solids particles start to move under the same air velocity. When the solid particles are dried for 40 minutes, liquid film on the particle surface nearly evaporates and the increase rate of correlation velocity decreases. With further drying, the water in the pores of the particle evaporates and the weight of the particle reduces, thus the spatial-averaged correlation velocity in the FBD still increases.

Figure 11. Weighted average velocity from different electrode sets when the moisture content is 12.2 wt. % under the experimental condition of TC3.

Figure 12. Spatial-averaged correlation velocity during the drying process under the experimental condition of TC3.

4.4. Moisture content measurement

In order to measure the moisture content in the FBD, a predictive model is proposed using the average RMS value of the electrostatic signals from the twelve electrodes in the sensor array. The moisture content (X) during the drying process is determined from

$$X = X_0 - aA_{rms}{}^b \tag{2}$$

where X_0 is the initial moisture content, A_{rms} is the average RMS value of the electrostatic signals and a and b are coefficients. Since the initial moisture content and the moisture contents at different sampling times are known, the above equation can be simplified as

$$\Delta X = a \times A_{rms}{}^b \tag{3}$$

The coefficients a and b in the equation are determined using least square method. For example, based on the experimental data under the air velocity of 0.52-0.57 m/s with different inlet air temperatures, the fitting of equation (3) is shown in Figure 13. The value of the coefficient of determination (R^2) for the fit is 0.93. The coefficients a and b under different air velocities are given in Table 2. It is found that the coefficient a is inversely related to the air velocity and the coefficient b can be determined by averaging the coefficients from different air velocities, which is set to 1.37.

Figure 13. Fitting of equation (3) based on the experimental data under the air velocity of 0.52-0.57

m/s with different inlet air temperatures.

Table 2. Coefficients of *a* and *b* under different air velocities

The spatial-averaged correlation velocity in the FBD can be measured using the electrostatic signals from the upstream and downstream electrodes in the sensor array and the coefficient *a* in the equation is formulated as

$$a = f(v_c) \tag{4}$$

where v_c is the correlation velocity determined by the weighted average cross-correlation. Based on the results of correlation velocity and the coefficient *a*, a power exponent fit is conducted, as shown in Figure 14, and the R^2 for the fit is 0.99. As a result, the coefficients *a* and *b* in equation (3) are determined and the moisture content during the drying process can be predicted using the electrostatic signals from the sensor array. The advantage of the proposed method is that the solids moisture is predicted only from measurements of the electrostatic sensor array.

Figure 14. Fitting of coefficient *a* and correlation velocity v_c.

The moisture content of solid particles predicted using the electrostatic signals and the moisture content obtained from the samples are compared, as shown in Figure 15. During the experiment, when the moisture content went below 11 wt.%, the voltage of the electrostatic signal exceeded the higher limit of the measuring system and the calculated RMS value of the electrostatic signal was wrong. As a result, the predictions below 11 wt.% are not given in present paper. The statistical parameters of Root Mean Square Error (RMSE) and Mean Absolute Error (MAE) are applied to evaluate the performance of the predictive model.

$$RMSE = \sqrt{\frac{\sum_{i=1}^{n}(P_i - S_i)^2}{n}} \tag{5}$$

$$MAE = \frac{\sum_{i=1}^{n}|P_i - S_i|}{n} \tag{6}$$

where P_i and S_i are the predicted value and the sampled value, respectively. The RMSE of the model under different air velocities are 0.28, 0.45 and 0.95, respectively. The MAE of the model under

different air velocities are 0.23, 0.39 and 0.79, respectively. It is found that the disparity between the predicted value and the sampled value increases with the air velocity. The reason for this result is that when the air velocity increases, the flow in the FBD becomes more turbulent and the particles from the sampling port cannot represent the actual moisture content in the whole FBD. However, from the results shown in Figure 15, it is demonstrated that the predicted values using the electrostatic signals from the sensor array are within ±15% of the moisture content from the sampled particles.

Figure 15. Moisture content predicted using the electrostatic signals under different air velocities.

5. Conclusions

Due to the advantages of non-intrusiveness to the flow, high sensitivity and on-line continuous measurement, an electrostatic sensor array has been arranged in the dense phase region of a lab-scale FBD to measure the moisture content during the drying process. Although there is no theoretical relationship between the moisture content and the electrostatic charge, it has been found that the fluctuation of the electrostatic signal can reveal the change in moisture content. However, the air velocity has a significant impact on the relationship between the RMS value of the electrostatic signal and the moisture content in the bed. By taking the velocity effect into account, a predictive model for the measurement of moisture content using the average RMS value of the electrostatic signals has been formulated. The RMSE and MAE between the predicted and the sampled values have been determined and compared. The results have demonstrated that the model can predict the moisture content with reasonable accuracy. It is envisaged that, with the knowledge of moisture content in the FBD, the drying process can be controlled and optimized under variable operating conditions.

Acknowledgments

The authors wish to acknowledge the National Natural Science Foundation of China (No. 61403138) and Beijing Natural Science Foundation (No. 3162031).

References

[1] W.R.W. Daud, Fluidized bed dryers — recent advances, Adv. Powder Technol. 19 (2008) 403–418.

[2] Y. Su, M. Zhang, A.S. Mujumdar, Recent developments in smart drying technology, Dry. Technol. 33 (2015) 260–276.

[3] G. Chaplin, T. Pugsley, C. Winters, Application of chaos analysis to pressure fluctuation data from a fluidized bed dryer containing pharmaceutical granule, Powder Technol. 142 (2004) 110–120.

[4] G. Chaplin, T. Pugsley, C. Winters, The S-statistic as an early warning of entrainment in a fluidized bed dryer containing pharmaceutical granule, Powder Technol. 149 (2005) 148–156.

[5] H. Tsujimoto, T. Yokoyama, C.C. Huang, I. Sekiguchi, Monitoring particle fluidization in a fluidized bed granulator with an acoustic emission sensor, Powder Technol. 113 (2000) 88–96.

[6] L. Briens, R. Smith, C. Briens, Monitoring of a rotary dryer using acoustic emissions, Powder Technol. 181 (2008) 115–120.

[7] S. Poutiainen, S. Matero, T. Hamalainen, J. Leskinen, J. Ketolainen, K. Jarvinen, Predicting granule size distribution of a fluidized bed spray granulation process by regime based PLS modeling of acoustic emission data, Powder Technol. 228 (2012) 149–157.

[8] F.N. Ihunegbo, C. Ratnayake, M. Halstensen, Acoustic chemometrics for on-line monitoring and end-point determination of fluidised bed drying, Powder Technol. 247 (2013) 69–75.

[9] G. Chaplin, T. Pugsley, Application of electrical capacitance tomography to the fluidized bed drying of pharmaceutical granule, Chem. Eng. Sci. 60 (2005) 7022–7033.

[10] H.G. Wang, W.Q. Yang, P. Senior, R.S. Raghavan, S.R. Duncan, Investigation of batch fluidized-bed drying by mathematical modeling, CFD simulation and ECT measurement, AICHE J. 54 (2008) 427–444.

[11] H.G. Wang, P.R. Senior, R. Mann, W.Q. Yang, Online measurement and control of solids moisture in fluidised bed dryers, Chem. Eng. Sci. 64 (2009) 2893–2902.

[12] V. Rimpilainen, L.M. Heikkinen, M. Vauhkonen, Moisture distribution and hydrodynamics of wet granules

during fluidized-bed drying characterized with volumetric electrical capacitance tomography, Chem. Eng. Sci. 75 (2012) 220–234.

[13] L. Chen, Y.H. Xie, C.H. Lin, S. Du, Experimental research on granule moisture measurement by microwave resonance technology in a fluidized bed dryer, Key Eng. Mater. 544 (2013) 466–470.

[14] F. Portoghese, F. Berruti, C. Briens, Use of triboelectric probes for on-line monitoring of liquid concentration in wet gas–solid fluidized beds, Chem. Eng. Sci. 60 (2005) 6043–6048.

[15] F. Portoghese, F. Berruti, C. Briens, Continuous on-line measurement of solid moisture content during fluidized bed drying using triboelectric probes, Powder Technol. 181 (2008) 169–177.

[16] W. Brennan, M. Jacobson, G. Book, C. Briens, L. Briens, Development of a tribolelectric procedure for the measurement of mixing and drying in a vibrated fluidized bed, Powder Technol. 181 (2008) 178–185.

[17] M. Aghbashlo, R. Sotudeh-Gharebagh, R. Zarghami, A.S. Mujumdar, N. Mostoufi, Measurement techniques to monitor and control fluidization quality in fluidized bed dryers: a review, Dry. Technol. 32 (2014) 1005–1051.

[18] A.H. Park, H.T. Bi, J.R. Grace, Reduction of electrostatic charges in gas-solid fluidized beds, Chem. Eng. Sci. 57 (2002) 153–162.

[19] A. Giffin, P. Mehrani, Effect of gas relative humidity on reactor wall fouling generated due to bed electrification in gas-solid fluidized beds, Powder Technol. 235 (2013) 368–375.

[20] X.C. Qian, D.P. Shi, Y. Yan, W.B. Zhang, G.G. Li, Effects of moisture content on electrostatic sensing based mass flow measurement of pneumatically conveyed particles, Powder Technol. 311 (2017) 579–588.

[21] M. Taghavivand, K. Choi, L. Zhang, Investigation on drying kinetics and tribocharging behaviour of pharmaceutical granules in a fluidized bed dryer, Powder Technol. 316 (2017) 171–180.

[22] X.C. Qian, X.B. Huang, Y.H. Hu, Y. Yan, Pulverized coal flow metering on a full-scale power plant using

electrostatic sensor arrays, Flow Meas. Instrum. 40 (2014) 185–191.

[23] X.C. Qian, Y. Yan, L.J. Wang, J.Q. Shao, An integrated multi-channel electrostatic sensing and digital imaging system for the on-line measurement of biomass–coal particles in fuel injection pipelines, Fuel 151 (2015) 2–10.

[24] W.B. Zhang, Y.P. Cheng, C. Wang, W.Q. Yang, C.H. Wang, Investigation on hydrodynamics of triple-bed combined circulating fluidized bed using electrostatic sensor and electrical capacitance tomography, Ind. Eng. Chem. Res. 52 (2013) 11198–11207.

[25] W.B. Zhang, Y. Yan, Y.R. Yang, J.D. Wang, Measurement of flow characteristics in a bubbling fluidized bed using electrostatic sensor arrays, IEEE Trans. Instrum. Meas. 65 (2016) 703–712.

[26] Y. Yang, Q. Zhang, C. Zi, Z.L. Huang, W.B. Zhang, Z.W. Liao, J.D. Wang, Y.R. Yang, Y. Yan, G.D. Han, Monitoring of particle motions in gas-solid fluidized beds by electrostatic sensors, Powder Technol. 308 (2017) 461–471.

[27] W.D. Greason, Investigation of a test methodology for triboelectrification, J. Electrostat. 49 (2000) 245–256.

[28] C. He, X.T. Bi, J.R. Grace, Simultaneous measurements of particle charge density and bubble properties in gas-solid fluidized beds by dual-tip electrostatic probes, Chem. Eng. Sci. 123 (2015) 11–21.

[29] C. He, X.T. Bi, J.R. Grace, Decoupling electrostatic signals from gas-solid bubbling fluidized beds, Powder Technol. 290 (2016) 11–20.

[30] J.Q. Zhang, W.B. Zhang, Y.T. He, Y. Yan, Predicting the amount of coke deposition on catalyst pellets through image analysis and soft computing, Meas. Sci. Technol. 27 (2016) 114006.

[31] A.S. Mujumdar, Handbook of Industrial Drying 3 edition, CRC Press, 2006.

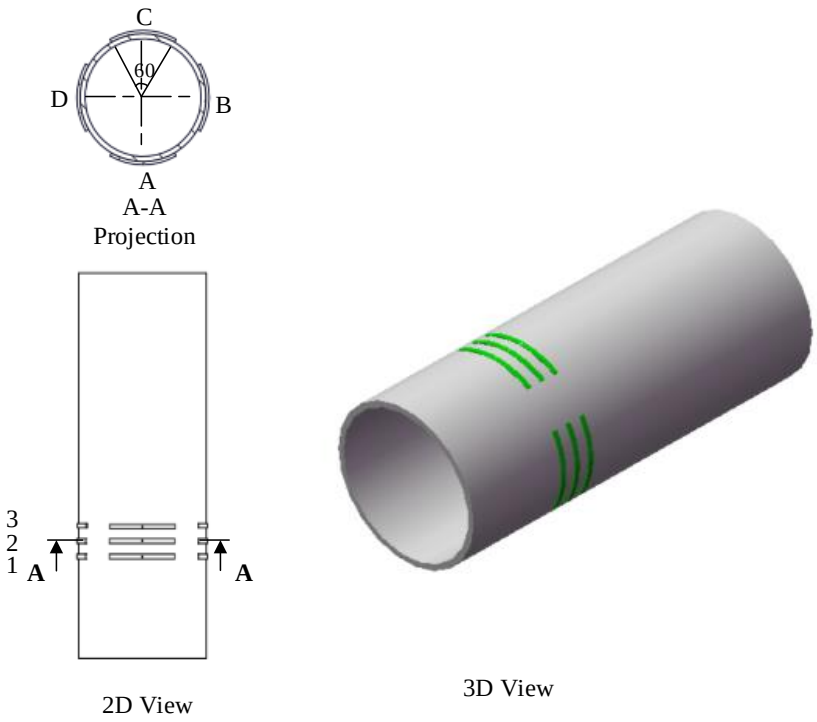

Figure 1. Electrostatic sensor array.

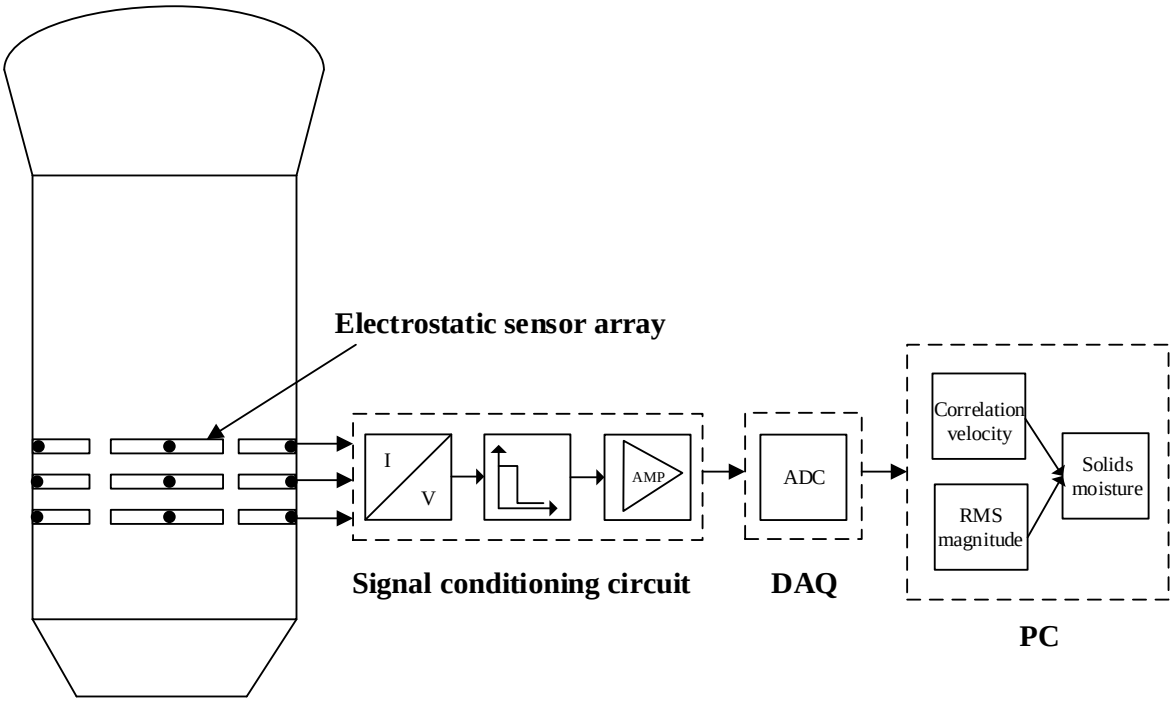

Figure 2. Signal conditioning and processing procedure of the electrostatic sensor array.

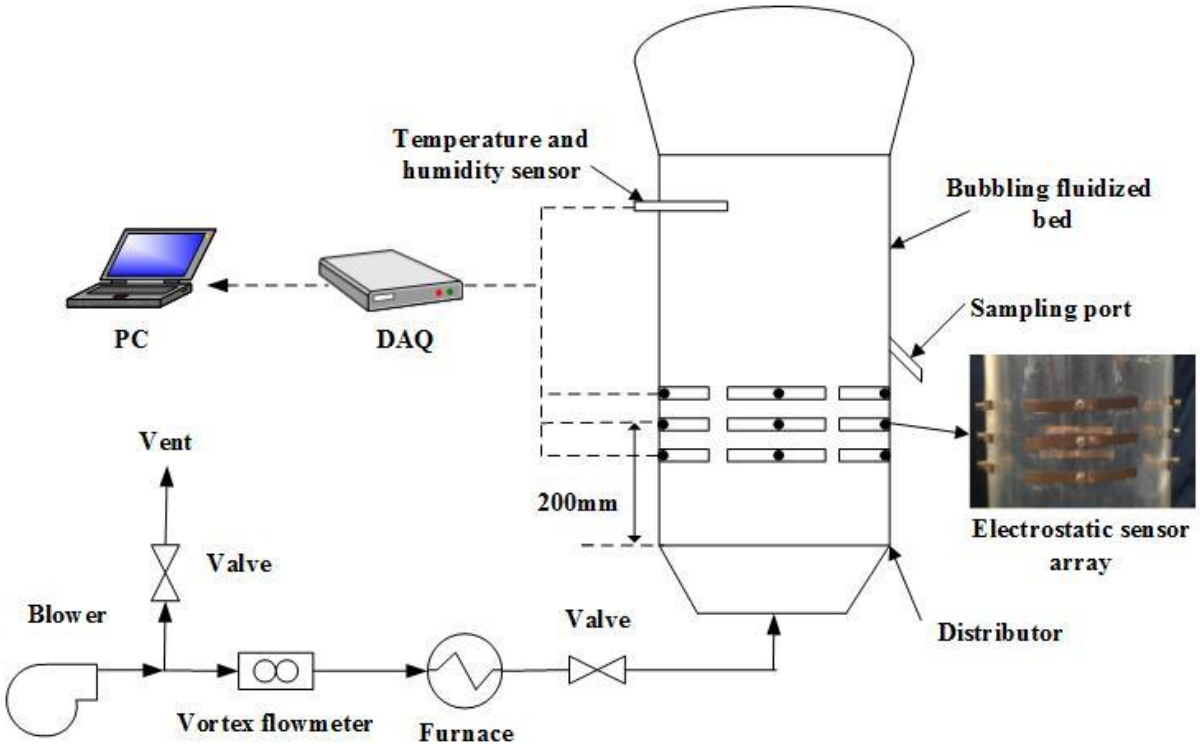

Figure 3. Experimental setup of the fluidized bed dryer.

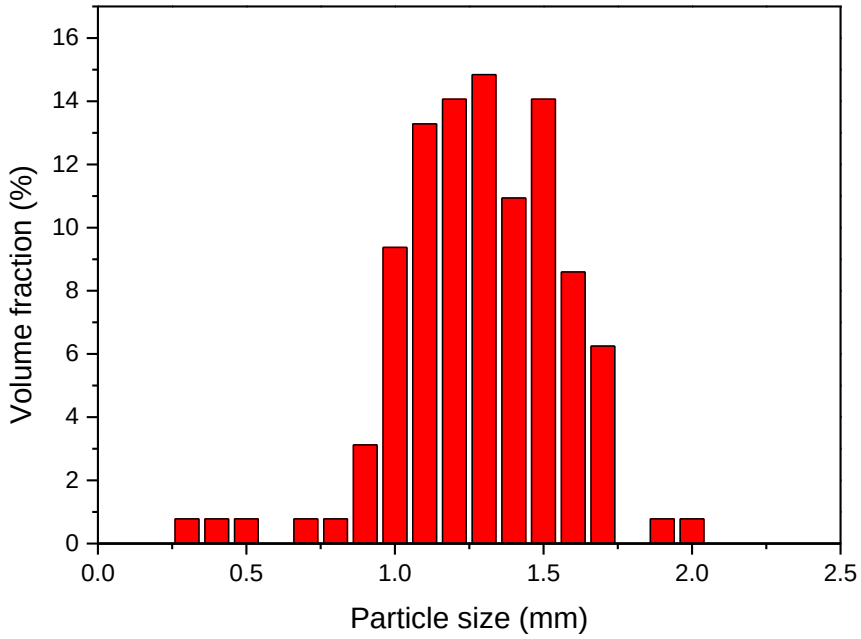

Figure 4. Size distribution of the corn particles.

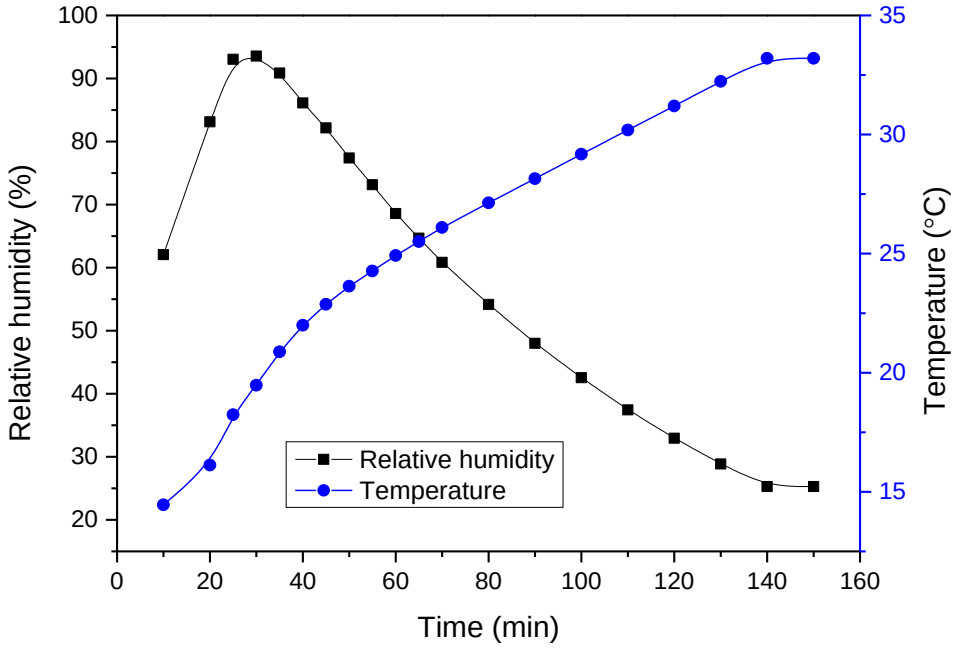

Figure 5. Temperature and relative humidity of the exhaust air during the drying process under the experimental condition of TC3

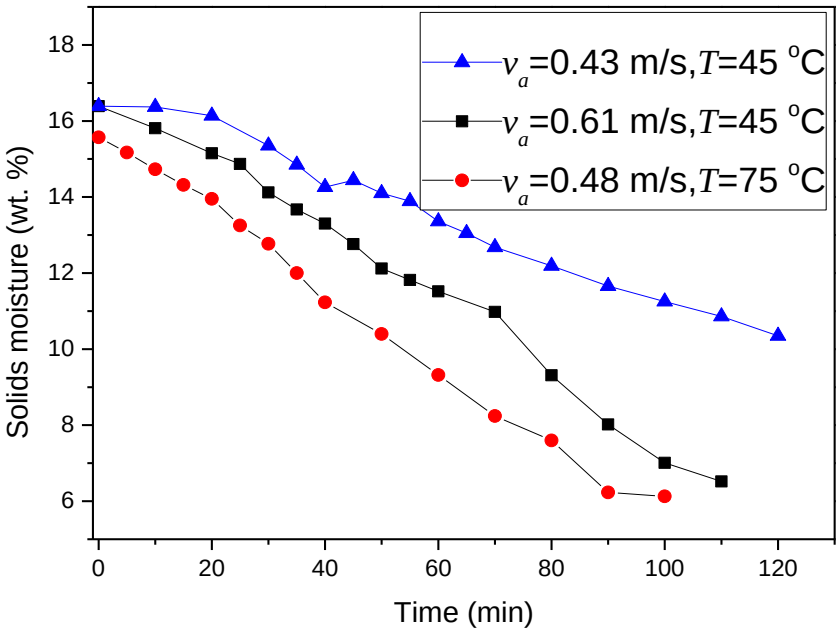

Figure 6. Time history of moisture content under different conditions.

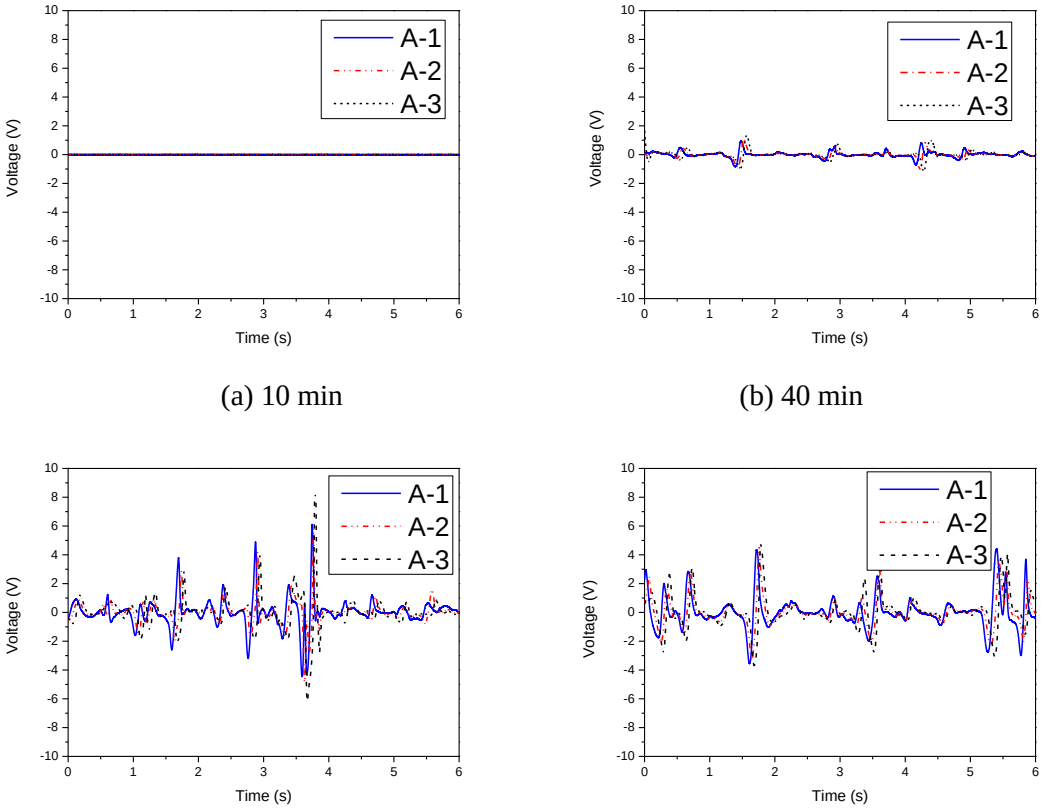

(a) 10 min (b) 40 min

(c) 70 min (d) 100 min

Figure 7. Electrostatic signals from electrodes A-1, A-2 and A-3 during the drying process under the experimental condition of TC3.

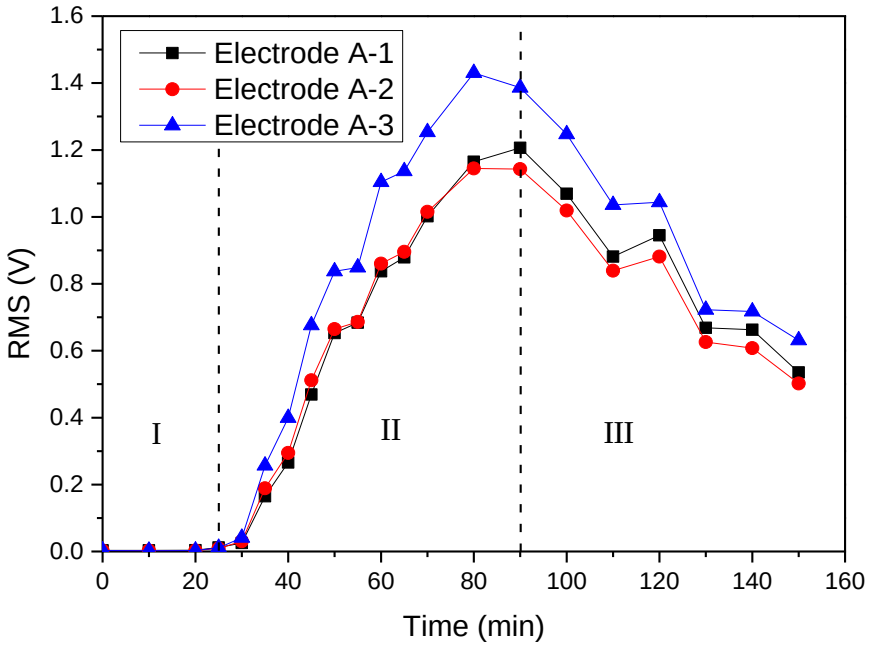

Figure 8. RMS values of the electrostatic signals from set A electrodes during the drying process under the experimental condition of TC3.

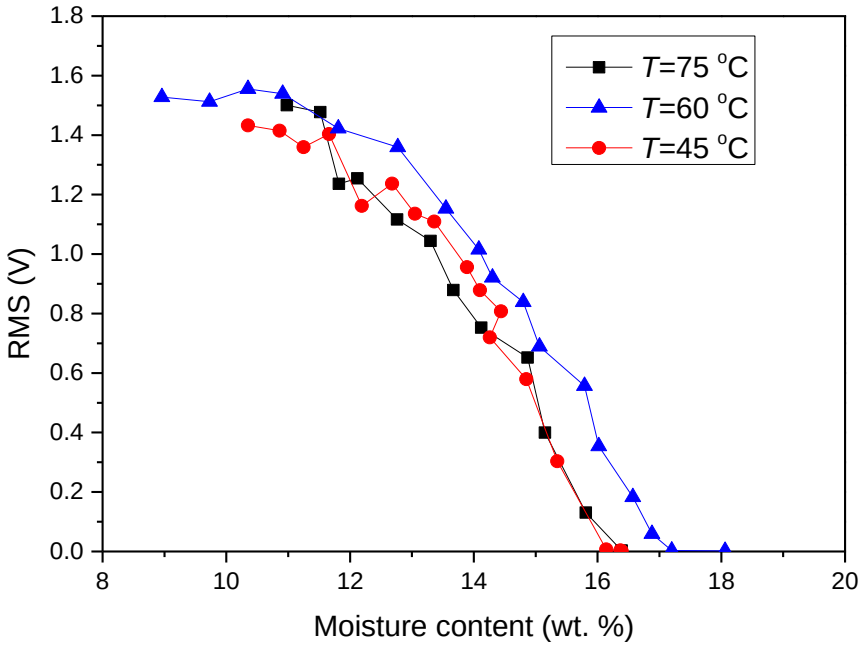

Figure 9. Relationships between the average RMS value of the electrostatic signals and the moisture content under the air velocity of 0.52-0.57 m/s with different inlet air temperatures.

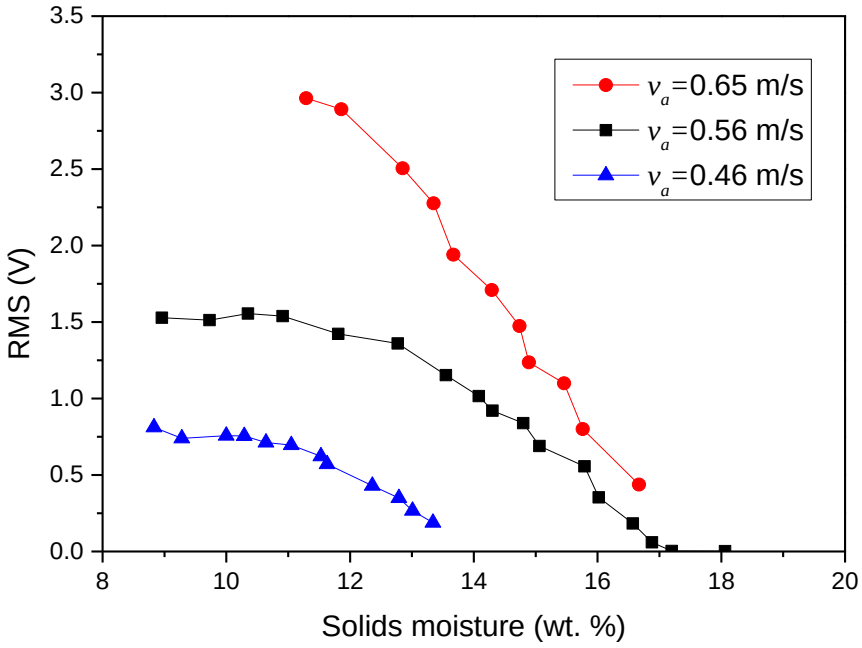

Figure 10. Relationship between the average RMS value of the electrostatic signals and the moisture content under the same inlet air temperature of 60 ^{o}C with different air velocities

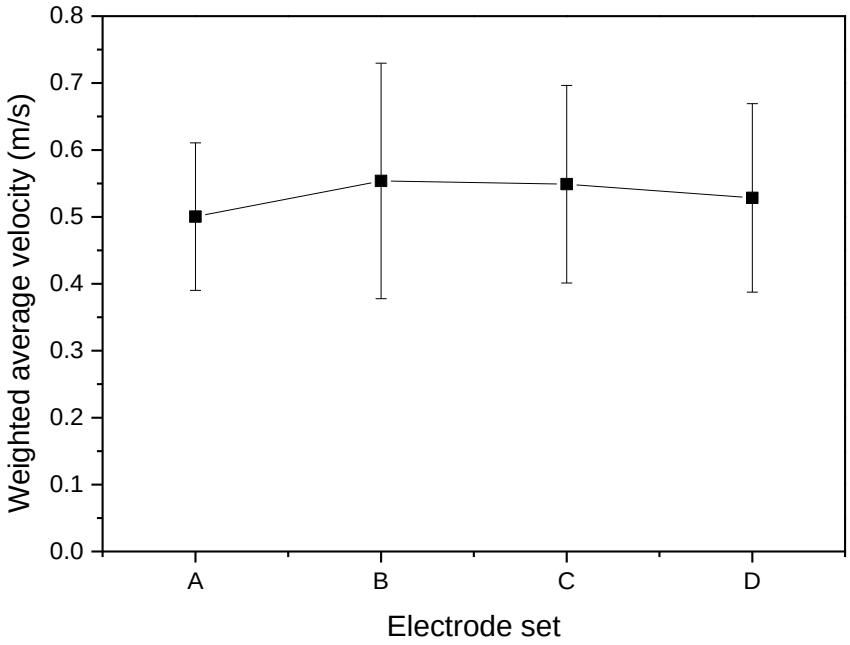

Figure 11. Weighted average velocity from different electrode sets when the moisture content is 12.2 wt. % under the experimental condition of TC3.

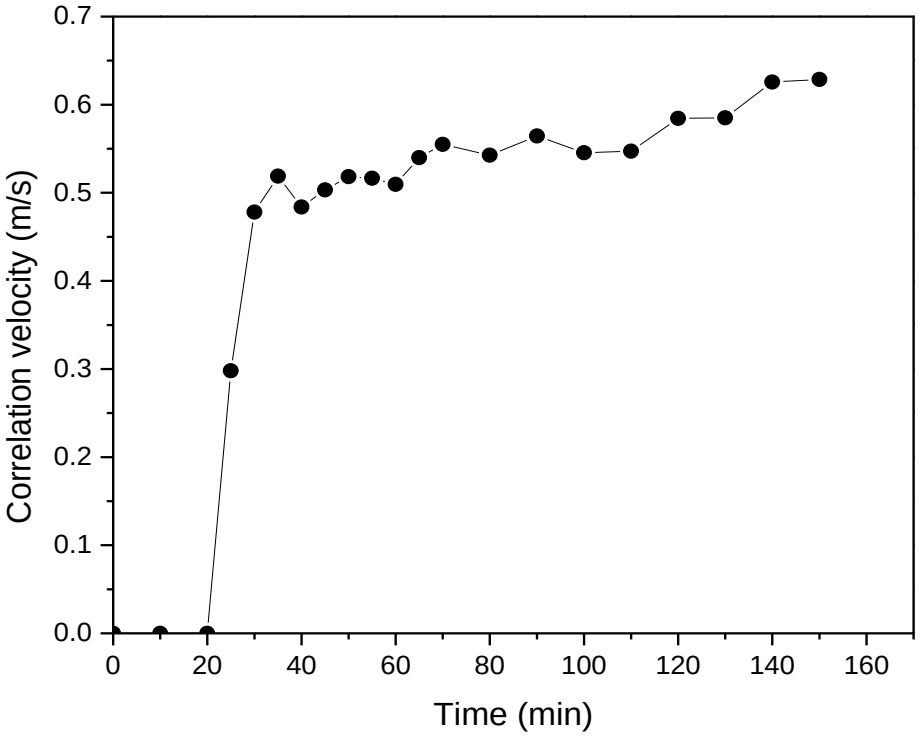

Figure 12. Spatial-averaged correlation velocity during the drying process under the experimental condition of TC3.

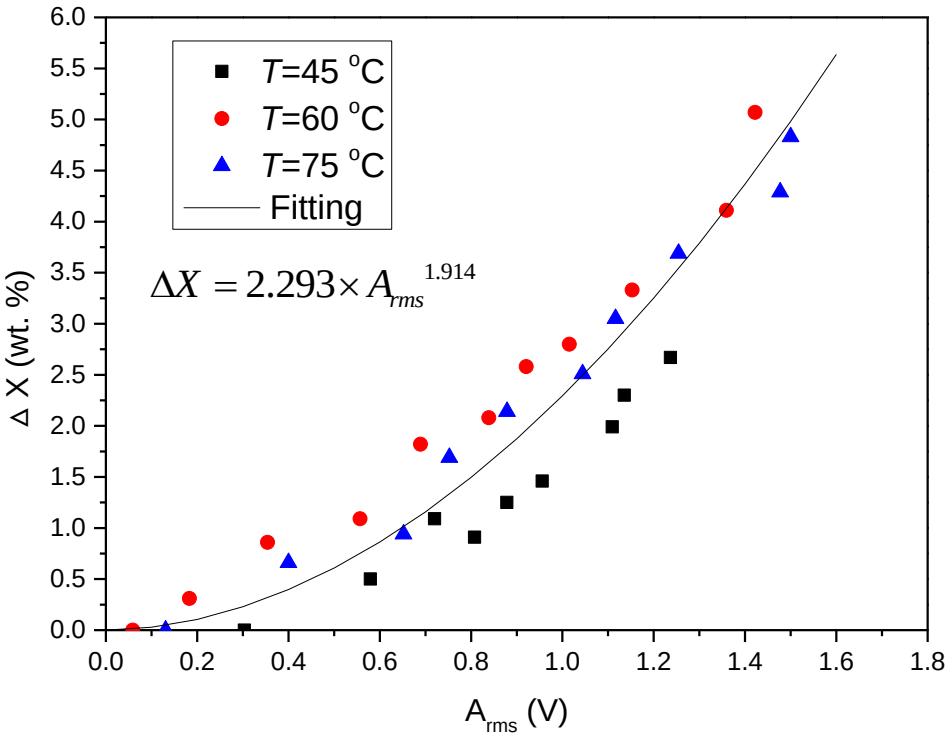

Figure 13. Fitting of equation (3) based on the experimental data under the air velocity of 0.52-0.57 m/s with different inlet air temperatures.

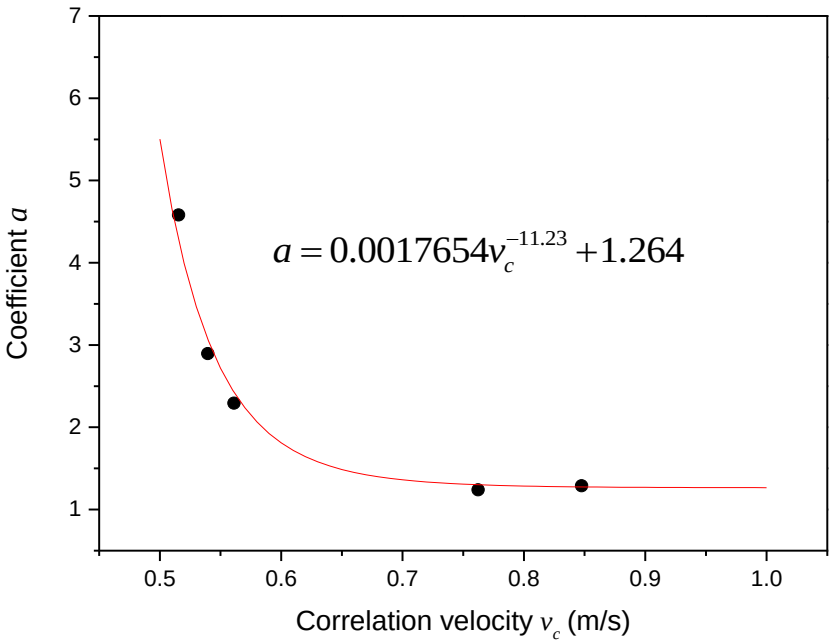

Figure 14. Fitting of coefficient *a* and correlation velocity v_c.

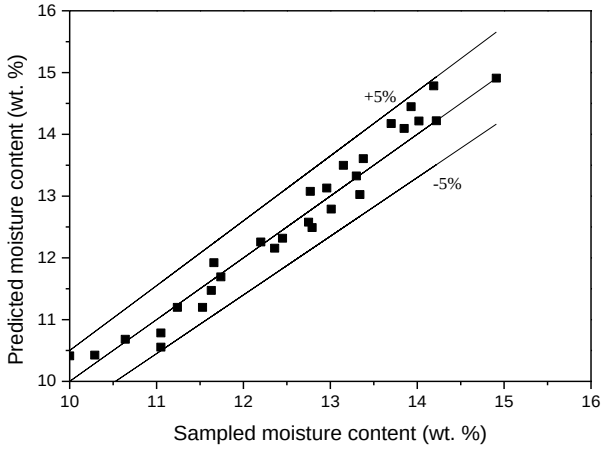

(a) Air velocity of 0.43-0.48 m/s

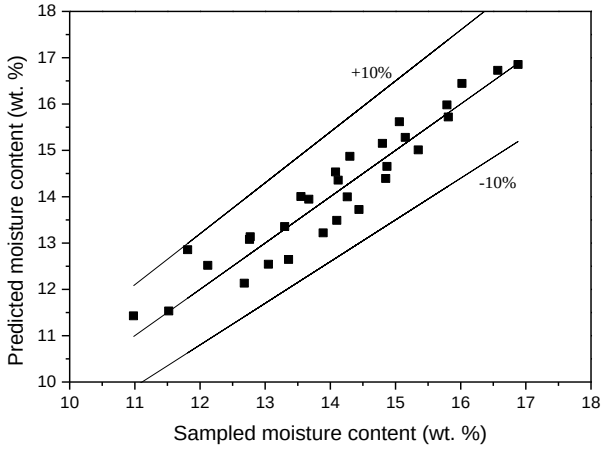

(b) Air velocity of 0.52-0.57 m/s

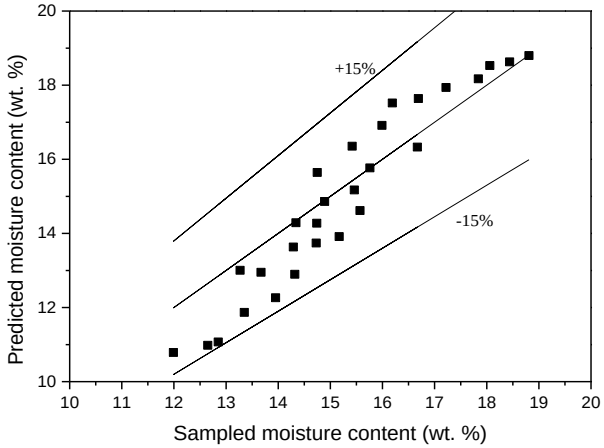

(c) Air velocity of 0.61-0.67 m/s

Figure 15. Moisture content predicted using the electrostatic signals under different air velocities

Table 1. Experimental conditions of the fluidized bed dryer under different inlet air velocities and air temperatures

Air velocity (m/s)	**Air temperature (°C)**		
	45	**60**	**75**
0.43-0.48	TC1	TC2	TC3
0.52-0.57	TC4	TC5	TC6
0.61-0.67	TC7	TC8	TC9

Table 2. Coefficients of *a* and *b* under different air velocities

Air velocity (m/s) (Temperature 60 ºC)	***a***	***b***
0.46	4.580	1.531
0.52	3.644	0.845
0.56	2.293	1.914
0.59	1.395	1.198
0.65	1.288	1.362